An Electrochemical Coulomb Staircase: Detection of Single Electron-Transfer Events at Nanometer Electrodes

Fu-Ren F. Fan and Allen J. Bard*

The current-potential curve at a 2.8-nanometer-radius electrode immersed in a solution containing micromolar concentrations of a redox couple, [(trimethylammonio)methyl] ferrocene (Cp_2FeTMA^+)/Cp_2FeTMA^{2+}, shows discrete steps (a coulomb staircase) representing single electron-transfer events. Discrete potential steps are also found in the current-time curve as the electrode potential relaxes back to equilibrium after a coulostatic potential step.

We describe electrochemical current-potential (*i-V*) curves at nanometer-size electrodes that are characterized by stepwise changes in current (rather than the usual smooth curves found at larger electrodes). These represent single electron-transfer events occurring at an electrode in an electrochemical cell. Earlier studies have shown that single molecules can be trapped and detected electrochemically at electrodes (*1*) and single reaction events of reactants generated at electrodes can be observed (*2*). We have previously discussed how single electron effects might be detectable at the electrode/solution interface (*3*). Typically, single electron effects have been studied with very small solid-state structures (such as quantum dots) where single electron charging and resonant tunneling through quantized energy levels regulate transport through the small structures (*4*). One of the simplest systems consists of two mesoscopic tunnel junctions in series, coupled through a quantum dot having a dimension on the order of 10 nm. When an external voltage scan is applied to this two-junction system, an *i-V* characteristic showing discrete steps is obtained (*5*–*8*). This coulomb staircase arises from the incremental increase in the current at voltages where it is energetically favorable for an additional electron to sit on the quantum dot. For room-temperature operation (*9*, *10*), the junction must be very small to ensure that the coulomb energy for one electron ($E_C = e^2/2C$) is greater than the thermal energy fluctuation, k_BT, where e is the electron charge, C is the junction capacitance, k_B is the Boltzmann constant, and T is the absolute temperature.

We achieve such a two-junction structure in an electrochemical system by using two nanometer-scale electrodes connected in series through a solution containing a redox couple. A schematic representation of two (electrode/solution) interfaces coupled in series through a solution and the setup for measurements is shown in Fig. 1. A voltage is applied between the electrodes, and the current flowing through the two-interface system is monitored in a current or voltage measurement mode with an electrometer (*11*). Each interface is characterized by a double-layer capacitance (C_d) and charge-transfer resistance (R_{CT}) and thus mimics a tunnel junction. The redox molecules in the solution serve as donors and acceptors for electron transfer and also as charge carriers for ionic conduction between two interfaces.

The Ir-Pt ultramicroelectrode used in this experiment was prepared by the procedures described previously (*12*). The size of the tip was determined from the steady-state tip current with the tip far away from a substrate, $i^0_{T,\infty}$, based on Eq. 1 (*13*)

$$i^0_{T,\infty} = 4nFDC^b a \qquad (1)$$

in which n is the number of electrons involved in the redox reaction {one for [(trimethylammonio)methyl]ferrocene (Cp_2FeTMA^+)}, F is the Faraday constant, D is the diffusion coefficient, C^b is the bulk concentration of Cp_2FeTMA^+, and a is the tip radius.

In Fig. 2, we show experimental data for a two-interface system consisting of two electrodes with radii of 2.5 and 3.2 nm about 2.5 cm apart in a solution containing 1 μM each of Cp_2FeTMA^+, Cp_2FeTMA^{2+}, NH_4^+, and SO_4^{2-}, and 2 μM PF_6^-. The *i-V* characteristic in the low-bias region (Fig. 2A) exhibits a staircase shape, and the differential conductance (*di/dV*) (Fig. 2B) consists of a series of peaks. The peak spacing, corresponding to the step width of the coulomb staircase, is 65 (±6) mV. The step heights of the staircase show some variation but were typically ~ 60 attoamperes (aA or 10^{-18} A). The general shape of the staircase was reproducible, although sharp changes in the current at some voltage locations sometimes occurred. The step width was independent of data sampling rate, voltage scan rate (<20 mV/s), and the concentration of the redox couple. The semiclassical model of the coulomb staircase takes account only of coulombic interactions and yields a peak spacing of (*6*, *7*)

$$\Delta V_{p\text{-}p} = e/C \qquad (2)$$

where C is the capacitance of the junction with the higher electron-transfer rate. The data in Fig. 2 give a calculated C of 2.4 (±0.2) × 10^{-18} F, which is close to the expected C_d of an electrode of radius 2.8 nm, if we assume a double-layer capacitance of 10 μF/cm². At a higher bias voltage (>0.3 V), the current attains a diffusion-limited plateau of about 530 aA, near that calculated from Eq. 1 under our experimental conditions (Fig. 2C). This corresponds to only about 3300 collisions per second of electroactive molecule (Cp_2FeTMA^+) with the electrode. A current staircase is observed in the low-bias region where the electron transfer is kinetically controlled.

A staircase *i-V* curve is also observed for another redox couple with the same pair of electrodes in a solution containing 10 μM $K_4Fe(CN)_6$ and 10 μM $K_3Fe(CN)_6$. The smoothed curve in Fig. 3A shows two steps between 0 and 0.14 V. The third and fourth steps (between 0.14 and 0.28 V) are not quite resolved and give an overall step of about twice the width and height as a one-electron process. The estimated step height for the $Fe(CN)_6^{4-}$/$Fe(CN)_6^{3-}$ couple is <7

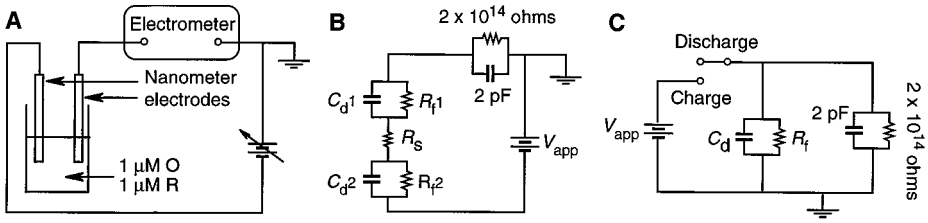

Fig. 1. (**A**) Experimental setup for the current or voltage measurements. (**B**) Schematic representation of two (electrode/solution) interfaces coupled in series through the solution. C_d, double-layer capacitance; R_f, faradaic impedance of each interface; R_s, solution resistance; V_{app}, voltage source. The electrometer has an input impedance of ~2 × 10^{14} ohms and a shunt capacitance of 2 pF. (**C**) Schematic representation of the experimental setup for the coulostatic experiment.

Department of Chemistry and Biochemistry, The University of Texas at Austin, Austin, TX 78712, USA.

*To whom correspondence should be addressed.

aA even though the concentration of the electroactive species is 10 times that of the ferrocene couple. The estimated staircase width is 0.07 ± 0.01 V, which is near the value seen with the ferrocene couple. This result is consistent with the predictions of the semiclassical coulomb staircase model and the much slower heterogeneous electron-transfer kinetics. On the basis of the semiclassical model of the coulomb staircase, the step height (Δi_{cs}) is, to the first approximation, inversely proportional to the charge transfer resistance, R_f, at the interface. R_f controls the charge-transfer kinetics of the electrochemical system, and Δi_{cs} is given by

$$\Delta i_{cs} = e/[R_f(C_d1 + C_d2)] \quad (3)$$

R_f at low overpotential is given by

$$R_f = (RT/F)[1/(nFAk_sC^b)] \quad (4)$$

in which R is the gas constant, k_s is the heterogenous electron-transfer rate constant, and A is the electrode area. Thus, the step height depends on A, k_s, C^b, and C_d, whereas the step width depends mainly on C_d as given by Eq. 2. The results shown here suggest that k_s for the $Fe(CN)_6^{4-}/Fe(CN)_6^{3-}$ couple is at least two orders of magnitude smaller than that for the $Cp_2FeTMA^+/Cp_2FeTMA^{2+}$ couple, which has a $k_s = 2.5$ cm/s as calculated from $\Delta i_{cs} = 60$ aA, $C_d1 + C_d2 = 4.4 \times 10^{-18}$ F, $C^b = 1$ μM, and $A = 2.0 \times 10^{-13}$ cm^2. The *i-V* curve for a pair of large Pt microdisk electrodes with radii of 5 and 12.5 μm is shown in Fig. 3B. The coulomb energy of one electron for electrodes of this size is very small (<50 nV), so that a smooth and linear response of the current as a function of voltage at low bias (for example, <0.3 V) is seen. At higher bias voltage, the current is expected to reach a diffusion-limited plateau.

Another approach to the single electron charging phenomenon is through a coulostatic-type experiment based on a single nanometer-size electrode (Fig. 1C). In this case, the other electrode was a saturated calomel electrode or a large Pt quasireference electrode (area, 0.2 cm^2). The two electrodes were immersed in a cell containing the $K_4Fe(CN)_6/K_3Fe(CN)_6$ redox couple. The nanometer-size electrode potential was displaced by about 85 mV from the equilibrium potential when this voltage was applied for 30 to 60 s between the two electrodes. After the applied voltage was switched off, the cell voltage, measured with a high input impedance electrometer, relaxed back to the equilibrium value. Because the electrometer input impedance is smaller than the faradaic impedance (*14*), the discharge of the cell voltage is governed by the input *RC* of the electrometer. In curve a of Fig. 4A, we show the observed uncorrected cell voltage (V_u) as a function of discharge time for an electrode (radius, 7 nm). A distorted staircase can be seen over an envelope of a smooth discharge background. In Fig 4A, curve b, the smooth discharge curve for a larger disk microelectrode (radius, 1 μm) is shown for comparison. This discharge curve is nearly coincident with the background discharge curve (V_m) associated with the shunt capacitance of the electrometer alone. V_u, after correction for V_m based on the relation $V_{corr} = 2V_u - V_m$ (*15*), is shown in Fig. 4B. As shown in Fig. 4B, when the discharge time is longer than 200 s, successive stepwise discharge steps become apparent and are clearly resolved. The step height was about 9 mV, in agreement with the expected change in the potential of an electrode of radius of 7 nm when it gains one electron. The step near the starting portion of the discharge curve (between 100 and 200 s) may be a two-electron step that is not well resolved. These data suggest that the temporal relation of the voltage of the electrochemical system, V_{corr}, can be represented as

$$V_{corr} = n(t)e/C + \text{terms independent of } n(t) \quad (5)$$

in which n is the discrete number of electrons gained by the electrode during the discharge process and C is its capacitance. This relation describes the discontinuous jump in V_{corr} during an electron-transfer event because the change in $n(t)$ is quantized. The step width progressively increases

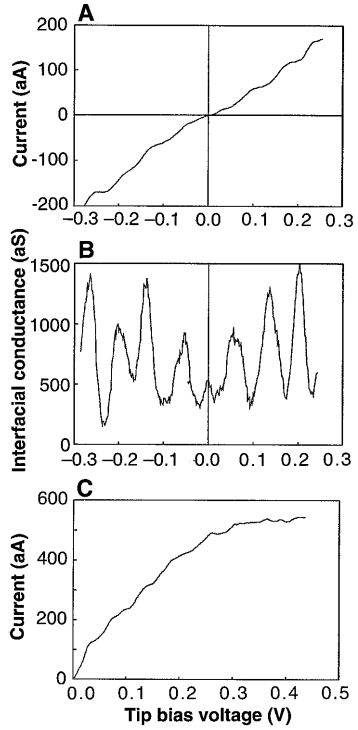

Fig. 2. (**A**) Experimental *i-V* characteristic of a two-interface system consisting of a pair of electrodes with radii of 2.5 and 3.2 nm immersed in a deaerated solution containing 1 μM each of Cp_2FeTMA^+, Cp_2FeTMA^{2+}, NH_4^+, and SO_4^{2-} and 2 μM PF_6^-. (**B**) The corresponding differential conductance (*di/dV*)-*V* plot. (**C**) *i-V* curve taken to more positive potentials.

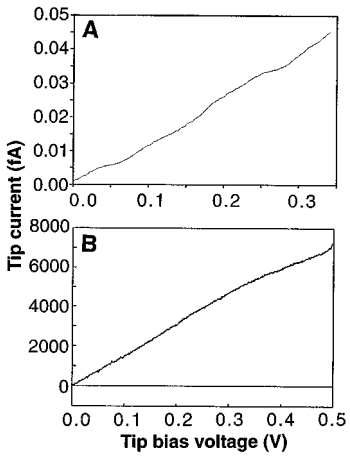

Fig. 3. (**A**) Smoothed experimental *i-V* characteristic of the same pair of electrodes as in Fig. 2 immersed in a deaerated solution containing 10 μM $K_4Fe(CN)_6$ and 10 μM $K_3Fe(CN)_6$. (**B**) Experimental *i-V* characteristic of a pair of microdisk electrodes (radii, 5 and 12.5 μm) in the same solution.

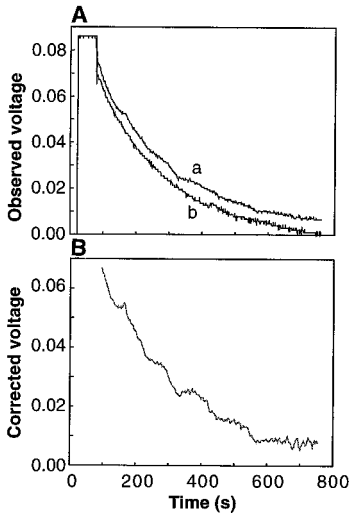

Fig. 4. (**A**) Curve a: Discharge curve (V_u) of an electrode (radius, 7 nm) in a deaerated solution containing 2 μM each of $K_4Fe(CN)_6$ and $K_3Fe(CN)_6$ after biasing at 85 mV versus the equilibrium cell voltage, V_0, for ~60 s. Curve b: The corresponding curve for a microdisk electrode (radius, 1 μm) (shifted down by 4.8 mV for clarity). (**B**) Corrected discharge curve (V_{corr}) based on the relation $V_{corr} = 2V_u - V_m$ (*15*). V_m is the background discharge curve of the shunt capacitance of the electrometer.

as the cell voltage decreases during discharge. The discharge behavior is governed here by the long time constant of the electrometer, but with slower redox couples it would also be governed by the heterogeneous electron-transfer kinetics. For example, at an electrode of radius a (nanometers) in a solution containing C^b (micromolar concentrations) redox couple with a heterogeneous electron-transfer rate constant k_s (centimeters per second), the number of net oxidative charge-transfer events, N_{CTE} (hertz), at low overpotential η, assuming the transfer coefficient $\alpha = 0.5$, is given by

$$N_{CTE} = 7.36 \times 10^2 a^2 k_s C^b \eta \qquad (6)$$

Thus for a 1 μM redox couple having slow charge-transfer kinetics, for example, k_s = 0.001 cm/s, it takes an average of ~25 s for a single electron-transfer event to occur at η = 9 mV at an electrode of radius 2.5 nm.

These coulomb staircase measurements show that nanometer-size structures can be produced without high-resolution lithographic processing or precise positioning of electrode tips. As with other single molecule processes, they may find use in the study of environmental effects on electron transfers and in determination of the heterogeneous kinetics of rapid electron-transfer reactions.

REFERENCES AND NOTES

1. F.-R. F. Fan and A. J. Bard, *Science* **267**, 871 (1995); F.-R. F. Fan, J. Kwak, A. J. Bard, *J. Am. Chem. Soc.* **118**, 9669 (1996).
2. M. M. Collison and R. M. Wightman, *Science* **268**, 1883 (1995).
3. F.-R. F. Fan and A. J. Bard, *Acc. Chem. Res.* **29**, 572 (1996).
4. Reviewed by H. Grabert and M. H. Devoret, Eds., *Single Charge Tunneling* (Plenum, New York, 1992); M. A. Kastner, *Phys. Today* **46**, 24 (January 1993).
5. I. O. Kulik and R. I. Shekhter, *Sov. Phys. JETP* **41**, 308 (1975).
6. M. Amman, R. Wilkins, E. Ben-Jacob, P. D. Maker, R. C. Jaklevic, *Phys. Rev. B* **43**, 1146 (1991).
7. A. E. Hanna and M. Tinkham, *ibid.* **44**, 5919 (1991).
8. M. Bockrath *et al.*, *Science* **275,** 1922 (1997).
9. R. P. Andres *et al.*, *ibid.* **272**, 1323 (1996).
10. L. Guo, E. Leobandung, S. Y. Chou, *ibid.* **275**, 649 (1997).
11. All current or voltage measurements were carried out at room temperature (25.0° ± 0.5°C) with a deaerated solution with a Keithley Model 617 electrometer. Current was found from the potential drop across the nominally 200-Tohm internal resistance at the most sensitive voltage setting. The leads were connected in the guard mode with the inner shield connected to the ungrounded electrode lead. The cell was placed inside a grounded Faraday cage.
12. L. A. Nagahara, T. Thundat, S. M. Lindsey, *Rev. Sci. Instrum.* **60**, 3128 (1989); M. V. Mirkin, F.-R. F. Fan, A. J. Bard, *J. Electroanal. Chem.* **328**, 47 (1992). Insulation of the tip was done with low–melting point polyethylene or Apiezon wax. The insulated tip was then mounted on a scanning electrochemical microscope (SECM) in a cell containing 1 mM Cp_2FeTMA^+ and 1 M $NaNO_3$. The very end of the tip was then exposed by applying 0.60 V versus saturated calomel electrode on the tip and −0.20 V on a conductive substrate (such as indium tin oxide, ITO) with the SECM operated in the constant current mode (with a reference current of 10 pA). As the well-insulated tip approached the surface of the substrate, the onset of an enhanced current flow caused the z-piezo to retract the tip. This process produced a hole in the tip insulation at the point of closest approach of tip to substrate while leaving most of the tip still insulated.
13. Y. Saito, *Rev. Polarogr.* **15**, 177 (1969).
14. A. J. Bard and L. R. Faulkner, *Electrochemical Methods* (Wiley, New York, 1980), p. 322.
15. Here we treat the electrochemical system (having a voltage V_{corr}) and the input shunt capacitor (having a voltage V_m) of the electrometer as two voltage sources coupled in parallel. Thus, the combined voltage (that is, the observed voltage V_u) is given by $(V_{corr} + V_m)/2$ or $V_{corr} = 2V_u - V_m$.

16. Supported by the Robert A. Welch Foundation and the National Science Foundation.

9 May 1997; accepted 22 July 1997

Solvophobically Driven Folding of Nonbiological Oligomers

James C. Nelson,* Jeffery G. Saven,† Jeffrey S. Moore, Peter G. Wolynes

In solution, biopolymers commonly fold into well-defined three-dimensional structures, but only recently has analogous behavior been explored in synthetic chain molecules. An aromatic hydrocarbon backbone is described that spontaneously acquires a stable helical conformation having a large cavity. The chain does not form intramolecular hydrogen bonds, and solvophobic interactions drive the folding transition, which is sensitive to chain length, solvent quality, and temperature.

Proteins and polynucleotides epitomize intramolecular self-organization in solution, as is evidenced by their spontaneous and reversible folding into well-defined conformations (*1*). A flexible biopolymer may assume many conformations, and entropic effects favor the absence of internal order. The folded state, however, is stabilized by a variety of noncovalent cohesive forces, including hydrogen (H) bonds, electrostatic forces, steric packing, and hydrophobic effects (*2*). Given the complexity of biopolymers, unraveling the respective roles of the entropic and energetic interactions remains a challenging area of theoretical (*3*) and experimental (*4*) research. Nonbiological macromolecules, however, may provide simpler systems for investigating self-organization and allow researchers to isolate particular interactions. In addition, the folding of linear polymers may provide synthetically simple means of generating architectures that could potentially rival the biopolymers in their complexity and functionality. One of the best studied folding motifs is the single-stranded helix, which can also serve as the basis for more complicated structures, as it does in proteins. In this report, we theoretically and experimentally characterize a nonbiological, supramolecular helix-forming oligomer.

Much emphasis has been placed on the role of H bonds in stabilizing secondary structures, ever since these structures were predicted in proteins on that basis (*5*). Many have argued that the primary reason that proteins fold is due to intramolecular H bonding of the backbone (*6*). Similarly, most attempts to create synthetic polymers with secondary structure have involved the engineering of H bonds, where the backbones used have been closely related to peptides (*7, 8*). However, H-bonded structures that are stable in nonpolar solvents often disintegrate in aqueous solution because of solvent competition (*7*). In proteins, hydrophobic interactions and compaction due to hydrophobic collapse undoubtedly also play a role in guiding helix formation (*9, 10*). Unlike H bonds, hydrophobic and van der Waals interactions are less selective and directionally specific, which discourages their use to confer conformational uniqueness. Given the substantial experimental focus on understanding H bonds in proteins and engineering them in synthetic polymers, we have chosen to investigate the extent to which nonspecific forces alone can guide intramolecular self-organization.

Although soluble ordered structures that are not largely H bonded have been obtained (*11*), here we report the folding of a phenylacetylene oligomer (Fig. 1A) whose cooperative transition can be driven, just as for proteins, by both solvent and temperature changes. The oligomer is guided to a folded, helical conformation by nondirectional interactions and local constraints caused by the covalent structure of the

J. C. Nelson and J. S. Moore, Departments of Chemistry and Materials Science and Engineering and the Beckman Institute for Advanced Science and Technology, University of Illinois, Urbana, IL 61801, USA.
J. G. Saven and P. G. Wolynes, School of Chemical Sciences, University of Illinois, Urbana, IL 61801, USA.

*Present address: Glaxo Wellcome, Five Moore Drive, Post Office Box 13398, Research Triangle Park, NC 27709, USA.
†Present address: Department of Chemistry, University of Pennsylvania, Philadelphia, PA 19104, USA.